Implementation of a digital optical phase conjugation system and its application to study the robustness of turbidity suppression by phase conjugation

Meng Cui[1]* and Changhuei Yang[1,2]

[1]Department of Electrical Engineering, California Institute of Technology, 1200 E. California Blvd., MC 136-93, CA, 91125, USA
[2]Department of Bioengineering, California Institute of Technology, 1200 E. California Blvd., MC 136-93, CA, 91125, USA
*mcui@caltech.edu

Abstract: In this work, we report a novel high capacity (number of degrees of freedom) open loop adaptive optics method, termed digital optical phase conjugation (DOPC), which provides a robust optoelectronic optical phase conjugation (OPC) solution. We showed that our prototype can phase conjugate light fields with ~3.9 x 10^{-3} degree accuracy over a range of ~3 degrees and can phase conjugate an input field through a relatively thick turbid medium ($\mu_s l$ ~13). Furthermore, we employed this system to show that the reversing of random scattering in turbid media by phase conjugation is surprisingly robust and accommodating of phase errors. An OPC wavefront with significant spatial phase errors (error uniformly distributed from $-\pi/2$ to $\pi/2$) can nevertheless allow OPC reconstruction through a scattering medium with ~40% of the efficiency achieved with phase error free OPC.

©2010 Optical Society of America

References and links

1. M. Wenner, "The most transparent research," Nat. Med. **15**(10), 1106–1109 (2009).
2. L. V. Wang, "Multiscale photoacoustic microscopy and computed tomography," Nat. Photonics **3**(9), 503–509 (2009).
3. I. M. Vellekoop, and A. P. Mosk, "Universal optimal transmission of light through disordered materials," Phys. Rev. Lett. **101**(12), 120601 (2008).
4. Z. Yaqoob, D. Psaltis, M. S. Feld, and C. Yang, "Optical phase conjugation for turbidity suppression in biological samples," Nat. Photonics **2**(2), 110–115 (2008).
5. I. M. Vellekoop, and A. P. Mosk, "Focusing coherent light through opaque strongly scattering media," Opt. Lett. **32**(16), 2309–2311 (2007).
6. I. M. Vellekoop, E. G. van Putten, A. Lagendijk, and A. P. Mosk, "Demixing light paths inside disordered metamaterials," Opt. Express **16**(1), 67–80 (2008).
7. M. Cui, E. J. McDowell, and C. H. Yang, "Observation of polarization-gate based reconstruction quality improvement during the process of turbidity suppression by optical phase conjugation," Appl. Phys. Lett. **95**(12), 123702 (2009).
8. M. Cui, E. J. McDowell, and C. Yang, "An in vivo study of turbidity suppression by optical phase conjugation (tsopc) on rabbit ear," Opt. Express **18**(1), 25–30 (2010).
9. A. Yariv, and P. Yeh, "Phase conjugate optics and real-time holography," IEEE J. Quantum Electron. **14**(9), 650–660 (1978).
10. J. Feinberg, and R. W. Hellwarth, "Phase-conjugating mirror with continuous-wave gain," Opt. Lett. **5**(12), 519–521 (1980).
11. R. C. Lind, and D. G. Steel, "Demonstration of the longitudinal modes and aberrationcorrection properties of a continuous-wave dye laser with a phase-conjugate mirror," Opt. Lett. **6**(11), 554–556 (1981).
12. I. Lindsay, "Specular reflection cancellation enhancement in the presence of a phase-conjugate mirror," J. Opt. Soc. Am. B **4**(11), 1810–1815 (1987).
13. D. M. Pepper, "Observation of diminished specular reflectivity from phase-conjugate mirrors," Phys. Rev. Lett. **62**(25), 2945–2948 (1989).

14. P. Yeh, *Introduction to photorefractive nonlinear optics* (John Wiley & Sons, Inc, New York, 1993).
15. D. P. M. Gower, *Optical phase conjugation* (Springer-Verlag, New York, 1994).
16. C. A. Primmerman, D. V. Murphy, D. A. Page, B. G. Zollars, and H. T. Barclay, "Compensation of atmospheric optical distortion using a synthetic beacon," Nature **353**(6340), 141–143 (1991).
17. M. J. Booth, M. A. A. Neil, R. Juskaitis, and T. Wilson, "Adaptive aberration correction in a confocal microscope," Proc. Natl. Acad. Sci. U.S.A. **99**(9), 5788–5792 (2002).
18. M. Rueckel, J. A. Mack-Bucher, and W. Denk, "Adaptive wavefront correction in two-photon microscopy using coherence-gated wavefront sensing," Proc. Natl. Acad. Sci. U.S.A. **103**(46), 17137–17142 (2006).
19. D. Débarre, E. J. Botcherby, T. Watanabe, S. Srinivas, M. J. Booth, and T. Wilson, "Image-based adaptive optics for two-photon microscopy," Opt. Lett. **34**(16), 2495–2497 (2009).
20. D. Débarre, E. J. Botcherby, M. J. Booth, and T. Wilson, "Adaptive optics for structured illumination microscopy," Opt. Express **16**(13), 9290–9305 (2008).
21. M. Fink, "Time reversed acoustics," Phys. Today **50**(3), 34–40 (1997).
22. M. Fink, "Time-reversed acoustics," Sci. Am. **281**(5), 91–97 (1999).
23. I. Yamaguchi, and T. Zhang, "Phase-shifting digital holography," Opt. Lett. **22**(16), 1268–1270 (1997).
24. T. Zhang, and I. Yamaguchi, "Three-dimensional microscopy with phase-shifting digital holography," Opt. Lett. **23**(15), 1221–1223 (1998).
25. A. Derode, A. Tourin, and M. Fink, "Random multiple scattering of ultrasound. Ii. Is time reversal a self-averaging process?" Phys. Rev. E Stat. Nonlin. Soft Matter Phys. **64**(3), 036606 (2001).
26. J. W. Goodman, "Some fundamental properties of speckle," J. Opt. Soc. Am. **66**(11), 1145–1150 (1976).

1. Introduction

In general, biological tissues are highly turbid media in the optical regime [1]. The extensive scattering of light by tissue is a significant obstacle for deep-tissue optical imaging and optical sensing [2]. In recent years, several publications [3–6] have reported that it is experimentally possible to mitigate the effects of scattering by tailoring an input light field wavefront appropriately. For example, Mosk's group showed that it is possible to focus light through a scattering medium by modifying and optimizing the wavefront of an input light field with a spatial light modulator [3,5]. Our group showed that an optical phase conjugate (OPC) copy of an initial transmission through a biological sample can likewise undo the effects of the initial scattering [4,7,8].

Employing optical phase conjugation to suppress tissue turbidity is appealing because it simply requires the duplication of a transmission light field for which the phase at each point on the wavefront is sign-reversed. Optical phase conjugation (OPC) has been an active field since the 1970s and has produced numerous applications including novel resonators, high-resolution image projection, and optical computing devices [9–15]. The generation of the OPC wave was based on optical nonlinearities such as photorefractive effect [14] and Brillouin scattering [15]. OPC based on nonlinear light-matter interactions can handle a large number of optical degrees of freedom. However, the nonlinear optics based OPC techniques often provide limited phase conjugation reflectivity, defined as the power ratio of the phase conjugate signal to the input signal. In addition, specialized light source and nonlinear media are usually required [15]. For practical purposes, an OPC system that can work with various light sources of different wavelengths, coherence lengths, and power levels would be preferable.

Another promising class of optical methods is adaptive optics. In adaptive optics, a wavefront sensor and modulator are used to measure and compensate for phase aberration. Adaptive optics techniques were originally developed to compensate for atmospheric distortion in astronomical telescopes [16]. In the past two decades, several research teams have employed adaptive optics techniques to compensate for the aberration in the optical microscopy systems and the aberration induced by the refractive index variation in the specimen [17–19]. The amount of aberration in these applications is fairly limited and can often be decomposed to several orders of Zernike polynomials [17–20]. In such cases, deformable mirrors are often employed as the wavefront modulator to provide adequate aberration compensation. Recently Mosk's team has successfully demonstrated a pixel by pixel optimization method to form an optical focus through highly turbid samples ($\mu_s l$ ~10, μ_s, scattering coefficient, l, sample thickness) by using high capacity spatial light modulators [3].

In this work, we present a high capacity (10^6 degrees of freedom) open loop adaptive optics method, named digital optical phase conjugation (DOPC), to achieve fast phase conjugation through a turbid medium ($\mu_s l$ ~13). Comparing to nonlinear optics based OPC

systems, DOPC has two significant advantages. First, as an adaptive optics method, the power of the generated OPC wave is independent of the input signal and can be freely adjusted. Second, the same DOPC system can in principle work with both CW and pulsed laser systems at any power levels. Both of these two properties are highly desired for biomedical applications. In addition, the optical degrees of freedom handled by DOPC are significantly greater than conventional adaptive optics methods [17,18] and is capable of achieving phase conjugation through highly turbid samples. As DOPC processes the entire wavefront simultaneously, it is inherently a fast wavefront optimization process and is potentially suitable for *in vivo* biomedical applications.

Since the wavefront is digitally controlled in the DOPC system, we can also use the DOPC system to study the fundamental properties of phase conjugation through random scattering media. One specific problem that the DOPC system is uniquely suited to tackle is the question of how tolerant the process of optical phase conjugation (OPC) through a random scattering media is to phase errors in the phase conjugation wavefront. The DOPC system allows us to introduce phase errors into the wavefront in a well-controllable fashion. Using our prototype, we experimentally found that, counter to intuition, OPC through random scattering media is surprisingly robust in the presence of significant phase errors. Our experimental findings are in good agreement with predictions derived from transmission matrix formulism [3].

In Section 2, we introduce the design of the DOPC system. In Section 3, we discuss the experimental implementation of the DOPC system and its calibration method. In Section 4, we show the experiment that was used to test the accuracy of the DOPC system. In Section 5, we discuss the experiments, in which we used the DOPC system to reconstruct an optical mode through a turbid medium ($\mu_s l$ ~13). In Section 6, we analyze the influence of phase errors on the phase conjugation signal through random scattering media and present experimental results.
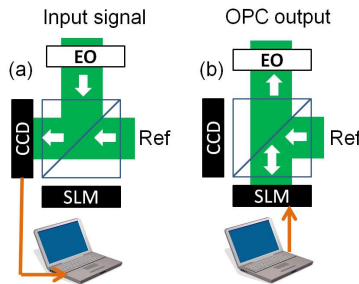
Fig. 1. The two elements of the DOPC system, a wavefront measurement device (sensor) and a spatial light modulator (actuator), are optically combined with a beam splitter. They function as a single system which can both measure an input wavefront and generate a phase conjugate output wavefront. (a) shows the wavefront measurement process wherein a reference wave interferes with the input signal. Their relative phase is controlled by an EO phase modulator. (b) shows the phase shaping process wherein the SLM modulates the incident reference wave.

2. Design

To generate phase conjugate wave digitally, we simply need a device which can be used both as a sensor and as an actuator. The piezo transducer employed in acoustic time reversal experiments is a good example [21,22]. Unfortunately, such a device does not currently exist for optical processing. We can potentially implement an equivalent system by combining a wavefront measurement device (sensor) with a spatial light modulator (SLM, actuator) in an optical arrangement as shown in Fig. 1. Such a composite system should work if the two components are exactly aligned with respect to each other so that each device forms a virtual image on the other device. In other words, we want every pixel of the sensor to form a virtual image on a corresponding pixel of the actuator, and vice versa. We name this approach digital optical phase conjugation (DOPC) because it is optoelectronics in nature.

Figure 1 illustrates the design of the DOPC system, in which a 50:50 beam splitter is employed to form virtual images between a CCD camera and a SLM. The generation of an OPC wave takes place in two steps. In step 1, the beam splitter directs the input signal towards the CCD camera. A reference wave with a flat wavefront is provided to interfere with the unknown input wave and form a hologram on the CCD. The relative phase between the input and the reference is controlled by an electro-optic (EO) modulator. By using phase-shifting holography [23,24], we can uniquely determine the phase and amplitude information of the input wave. In step 2, the measured wavefront is digitally reversed by a computer and passed to the SLM. The reflection of the reference beam incident on the SLM is modulated and counter-propagates with respect to the input wave, which is the phase conjugate of the input signal.

The advantages of the DOPC system are: (1) the same system can be used for both CW and pulsed lasers; (2) the DOPC system can work flexibly at any wavelength and at any light intensity; (3) the power of the generated OPC wave is independent of the input signal and can be precisely controlled by a computer. With such a system, the OPC reflectivity, defined by the power ratio of the OPC signal to the input signal, can be freely controlled; (4) the operation of the DOPC system is open loop, requiring no iterative measurements or computations; (5) the large number of digitally controlled degrees of freedom allows us to flexibly alter the OPC wavefront. This last property is especially useful in helping us study the interaction of the OPC wave with the turbid medium.

3. Implementation

In this section, we discuss the experimental implementation of the DOPC system and its required calibration procedure, which ensures an accurate mapping between the measured wavefront and the SLM output.
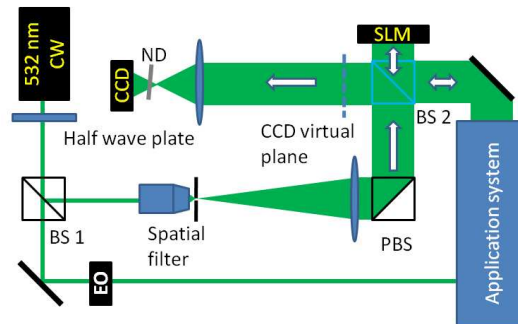
Fig. 2. Experimental setup of the DOPC system. The laser is a solid state CW laser at 532nm (Spectra-Physics, Excelsior Scientific 200mW). SLM, LCOS reflective spatial light modulator (Holoeye, LC-R 2500); CCD, CCD camera (ImagingSource DFK41BF02); PBS, polarizing beam splitter; BS1 and BS 2, non-polarizing beam splitter, ND, neutral density filter.

3.1 Setup

Figure 2 shows the experimental setup of the DOPC system. A solid state CW laser at 532nm (Spectra-Physics, Excelsior Scientific 200mW) was employed in the experiment. Its output first traveled through a half wave plate and was split to two beams by a non-polarizing beam splitter (BS 1). One beam traveled through an EO phase modulator and entered the application system. The other beam was spatially filtered and was used as the reference beam of the DOPC system. The reference beam was directed by a polarizing beam splitter (PBS) towards a non-polarizing beam splitter (BS 2) placed in front of a SLM (768 x 1024 pixels). Ideally, BS 2 should be placed at the symmetry plane between the SLM and the CCD and the SLM should form a mirror image onto the CCD, and vice versa. In practice, the size of the CCD pixel size was smaller than the SLM pixel size and we used a lens to form an enlarged image of the CCD at the symmetric position as shown by the "CCD virtual plane" in Fig. 2.

The SLM was mounted on a tilt and rotation platform driven by two differential micrometers (Newport, DM-13).
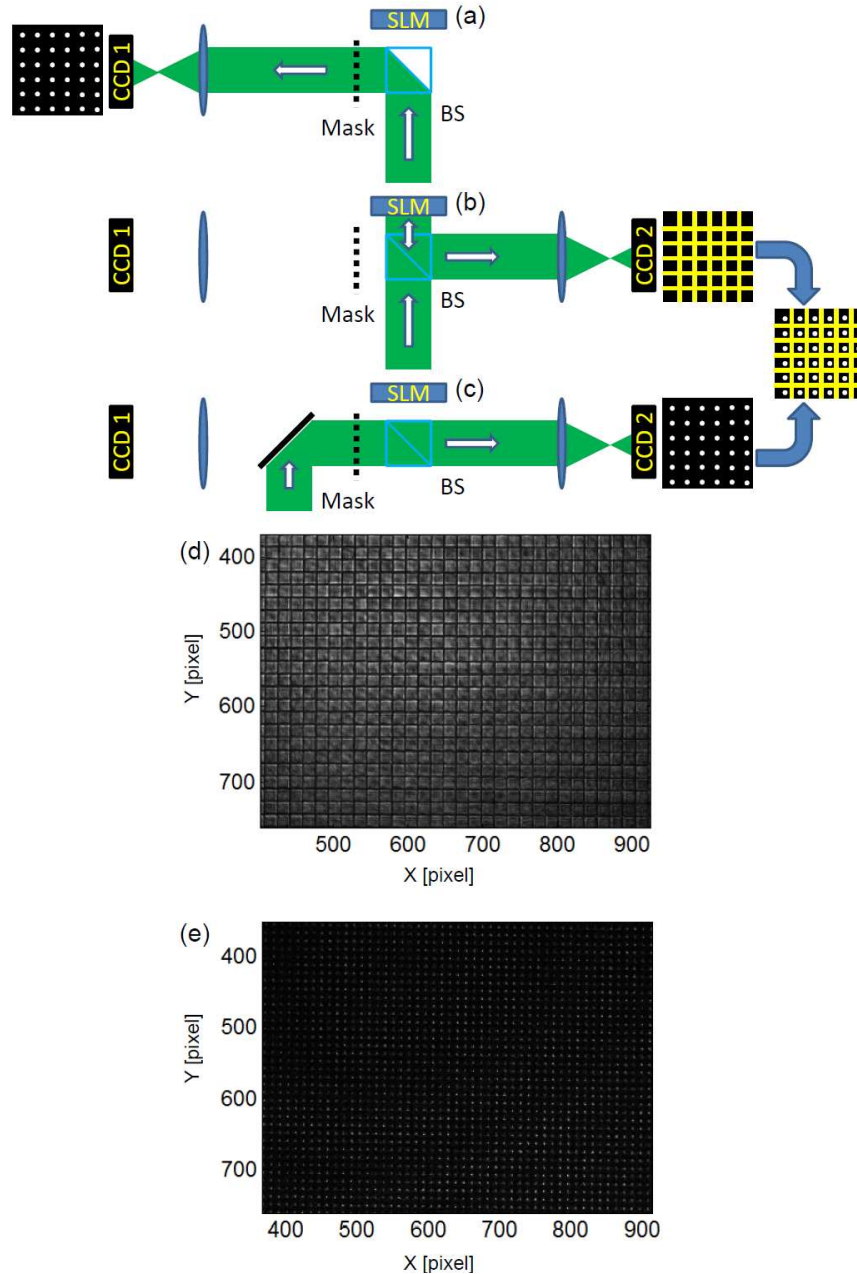
Fig. 3. The procedure for mapping between the CCD and the SLM. (a) A mask was placed at the symmetry plane of the SLM. The mask was illuminated and imaged on CCD 1. (b), a phase pattern was displaced on the SLM, which was imaged on CCD 2. (c) The mask was illuminated and was imaged on CCD 2. (d) Experimentally measured SLM image. (e) Experimentally measured mask image.

The input signal entered the DOPC system from right side of BS 2 and interfered with the reference beam to form a hologram on the CCD. The relative phase between the signal beam and the reference beam was modulated by the EO modulator. At the end of the phase-shifting holography, the phase information was retrieved by the computer from the holograms and

passed to the SLM that output the phase conjugate signal, a wave that counter-propagated with respect to the input signal with a reversed spatial phase profile. The power of the phase conjugate wave was determined by the power of the reference beam and was independent from the input signal, allowing us to arbitrarily control the phase conjugation reflectivity. We note that the input wave also entered the SLM and its reflection became a part of the output wave. Suppose the input signal is given by $E(x, y)\exp(i\phi(x, y))$. With the reversed phase profile $-\phi(x, y)$ displayed on the SLM, the reflected input signal by the SLM becomes $E(x, y)\exp(i\phi(x, y) - i\phi(x, y)) = E(x, y)$ that is a wave with a flat spatial phase profile, just as the reference wave. Experimentally, this signal was much weaker than the correctly shaped DOPC output.

During the wavefront measurement, a portion of the reference beam was reflected by the SLM and entered the application system. As long as the application system is not highly reflecting, this reflection does not significantly impact the wavefront measurement since this reflection is not phase modulated by the EO modulator. During the phase shaping, a portion of the reference beam was directed towards the CCD detector. We orientated the ND filter in front of the CCD such that the reflected light did not enter BS 2.

3.2 Calibration

The proper operation of the DOPC system requires that the CCD and SLM are correctly oriented with respect to each other, and that the phase measured by the CCD is appropriately mapped to the SLM. Since the reflection light field from the SLM does not actually falls on the CCD in the DOPC design, the alignment of the two elements cannot be trivially done. Instead, we have developed an alignment protocol that employs a sieve-like mask to serve as a referencing system during alignment. Our protocol is described below.

We first need to ensure that the SLM is perpendicular to the incident reference beam. To align the SLM, we measured the light that back-propagated through the spatial filter and BS 1 in Fig. 2, and maximized the back-propagating signal by adjusting the tilt and rotation platform carefully.
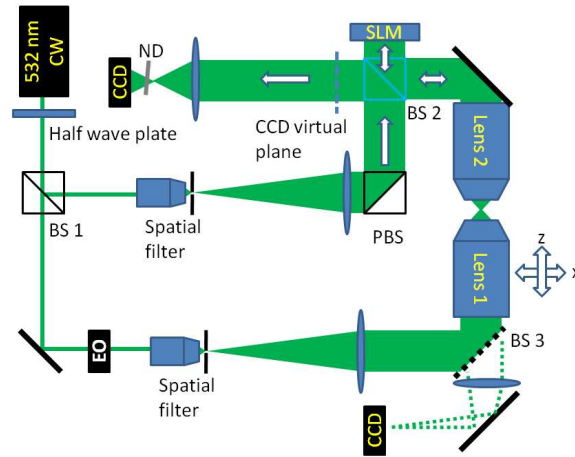
Fig. 4. Setup for testing the accuracy of DOPC. The laser is a solid state CW laser at 532nm. SLM, LCOS reflective spatial light modulator (Holoeye, LC-R 2500); CCD, CCD camera (ImagingSource DFK41BF02); PBS, polarizing beam splitter; BS, non-polarizing beam splitter. EO, electro-optic phase modulator (Thorlabs, EO-PM-NR-C4). Lens 1 and 2, objective lenses (Olympus, UPLFLN 100XO2, NA1.3), ND, neutral density filter.

The more challenging calibration step is the correct mapping of the wavefront measurement at the CCD to the SLM output. We developed a three-step procedure to address this issue. A chrome mask with 10 micron diameter holes and 20 micron hole spacing was made for the calibration. In step 1, we place the mask at the symmetry plane of the SLM as

shown in Fig. 3(a). The reflective mask and the SLM formed a Michelson interferometer. We set the phase of the SLM to 0 and adjusted the orientation of the mask while observing the interference pattern formed by the SLM and the mask. In such a way, we could make sure that the mask is parallel to the symmetry plane. The mask was mounted on a translation stage. We measured the distances from the SLM and the mask to the beam splitter and ensured that their difference was less than 0.5 mm. Since the SLM pixel size is ~20 micron and the Rayleigh range of a 532 nm Gaussian beam with 10 micron beam waist is greater than 1mm, a difference less than 0.5 mm is accurate enough for the purpose of calibration. We illuminated the mask and imaged the transmitted light onto CCD 1 which is the CCD camera used in DOPC experiment. In step 2, we illuminated the SLM and imaged the SLM onto another camera (CCD 2), as shown in Fig. 3(b). We divided the SLM into 64 x 48 blocks with 16 x 16 pixels in each block. The phase differences between adjacent blocks were set to π. Such an abrupt phase variation caused scattering. If the scattered light is not completely collected by the imaging system, the edges of the phase blocks would appear dark in the image, which was the case in our experiment. In such a way, we used phase shaping to produce an intensity pattern on the acquired SLM image. Figure 3(d) is an image of the SLM we experimentally acquired. In step 3, we illuminated the mask and imaged the transmitted light onto CCD 2, as shown in Fig. 3(c). Figure 3(e) is an image of the mask we acquired in step 3. By comparing the images acquired in step 2 and step 3, we know the relative position between the SLM pixels and the holes on the mask. The image acquired in step 1 informed us about the hole positions on CCD 1 that was the camera used in the actual DOPC experiment. In such a way, we can map the SLM pixels onto CCD 1.
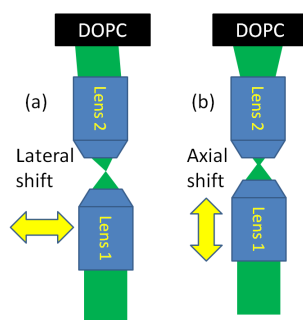
Fig. 5. (a) Lens 1 was shifted in the lateral direction. The beam exiting Lens 2 deviated from the original propagation direction. (b) Lens 1 was shifted in the axial direction. The beam incident on the DOPC system was either a converging or a diverging beam.

4. Experimental test

We next evaluated the performance of our DOPC system by examining its ability to accurately measure the light field from a point source and generate the phase conjugate field that can refocus at the point source .

4.1 Experiment setup

The experimental setup is shown in Fig. 4. To create a point source whose position can be controlled, we sent a spatially filtered beam through a NA 1.3 oil immersion objective lens (Lens 1) that was mounted a translation stage driven by differential micrometers (Newport, DM-13). The focused beam was collected by another identical objective lens (Lens 2) and directed to the DOPC system. The generated phase conjugate beam counter-propagated with respect to the input signal through Lens 2 and refocused at the point source. To measure the position accuracy and stability of the DOPC generated focus, we placed a beam splitter near the back aperture of Lens 1 and directed the transmitted phase conjugate beam towards a lens and focused the beam on a CCD detector. In the first test, we translated Lens 1 in the lateral direction, as shown in Fig. 5(a). In such a case, the beam exiting Lens 2 deviated from its original propagation direction. In the second test, we translated Lens 1 in the axial direction,

as shown in Fig. 5(b). In such a case, the beam exiting Lens 2 became either a diverging or a converging beam.
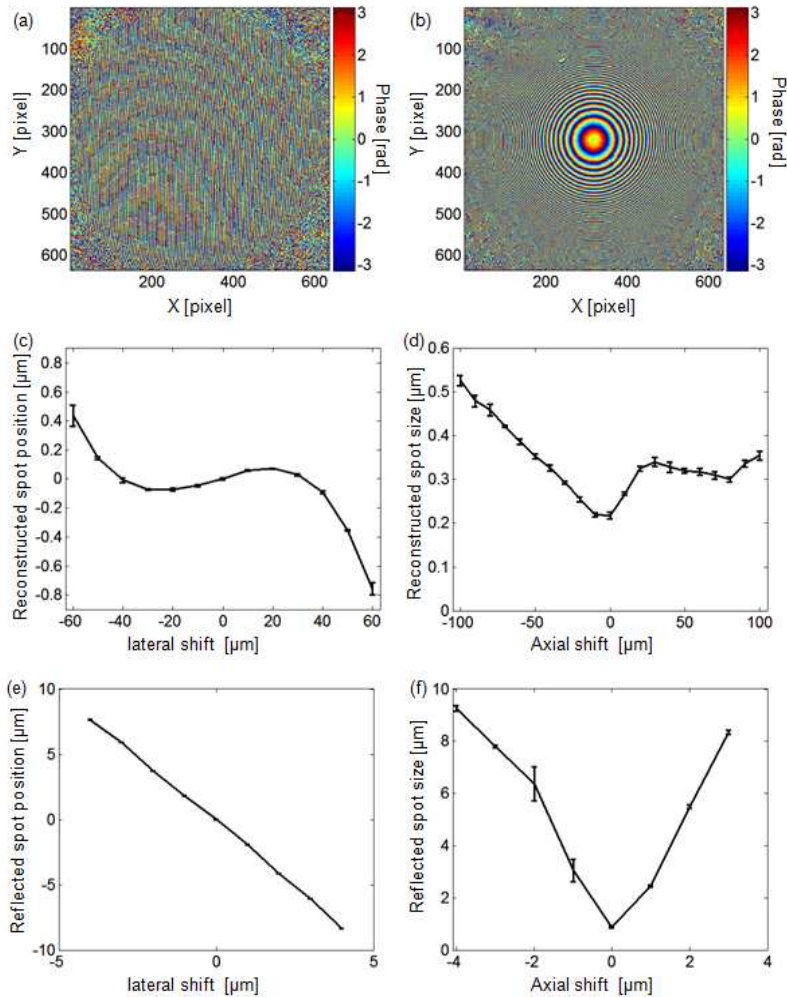
Fig. 6. (a) The phase shifting holography measured wavefront when lens 1 was shifted laterally from the center position by 50 microns. (b) The measured wavefront when Lens 1 was shifted axially from the center position by 50 microns. (c) The DOPC reconstructed focus position as Lens 1was shifted laterally. (d) The DOPC reconstructed focus diameter as Lens 1 was shifted axially. (e) The measured reflected focus position variation when Lens 1 was shifted laterally. (f) The reflected focus size variation when Lens 1 was shifted axially.

4.2 Results

We summarized the experimental results in Fig. 6. Figure 6(a) and 6(b) are the wavefronts measured by phase-shifting holography when Lens 1 was shifted by 50 microns laterally (a) and axially (b) from the centered position. The lateral displacement of Lens 1 caused the beam entering the DOPC system to deviate from the normal incidence angle on the SLM. Consequently, the measured phase had a constant slope in the lateral direction. Fourier analysis showed that there were ~2.5 pixels per 2π phase variation in Fig. 6(a). The axial displacement caused the beam entering the DOPC system to become either a converging beam or a diverging beam such that the phase slope gradually increased from the center to the outer area. Figure 6(c) shows the reconstructed focus position as Lens 1 was shifted from −60 to 60 microns. From −50 to 50 microns, the standard deviation from the center position is

~0.12 micron, which is small compared to the 0.23 micron focus diameter. Considering the 1.8 mm focal length of the 100x objective used in the experiment, we achieved a ~3.2 degree phase conjugation range with a ~3.9×10^{-3} degree accuracy. Figure 6(d) shows the reconstructed focus size as Lens 1 was shifted axially from −100 to 100 microns. We noticed that the spot size variation was asymmetric. In the case of negative axial displacement, the beam exiting Lens 2 was a diverging beam that could fill the entire SLM. The phase variation near the center was slow and could be accurately sampled and compensated by the DOPC system. The phase variation near the outer area of the SLM could exceed the sampling rate of the DOPC system and cause error. In the case of positive axial displacement, the beam exiting Lens 2 was a converging beam that could only fill the center area of the SLM. The high spatial frequency components were truncated by the objective lens, which caused the asymmetry in Fig. 6(d). As a comparison, we used a mirror to replace the DOPC system in Fig. 4 and performed the lateral and axial displacement experiments. Figure 6(e) shows the lateral displacement results. Linear fitting shows a slope of 1.99, which is expected since the angle deviation doubled upon reflection by the mirror. Figure 6(f) shows the axial displacement result. Without DOPC compensation, one micron displacement caused the reflected spot size to increase by more than tenfold to ~3 micron.

4.3 Compensation range of the DOPC system

The optical degrees of freedom of the DOPC system are limited by the pixel numbers of the SLM and the CCD camera. Given the number of pixels, we can estimate the amount of lateral displacement that can be compensated by the DOPC system. The SLM employed in our experiments has 768 x 1024 pixels that were mirrored onto an area on the CCD camera which contains slightly more pixels. In the experiments, 634 x 634 SLM pixels were imaged to the back aperture (~5mm in diameter) of the 100x objective lens. The maximum phase difference between adjacent pixels is π (Nyquist frequency), such that the total phase variation across the 634 pixels is 634π (317λ). The maximum angle deviation that can be compensated is therefore 317λ /5mm and the maximum lateral deviation at the focal plane is then $317\lambda f$/5mm, where f is the focal length of the objective. For an Olympus 100x objective, the focal length is ~1.8 mm and the theoretical maximum deviation from the center is therefore ~61 micron (λ = 532 nm). The experimentally achieved lateral compensation range in our system is ~50 micron.

5. Evaluation with a random scattering medium

A potential application of DOPC is to reconstruct an optical mode through a highly turbid medium. To demonstrate such a capability, and as a stringent test of our method, we apply the DOPC system to return an OPC wave through a scattering medium of $\mu_s l$ ~13.
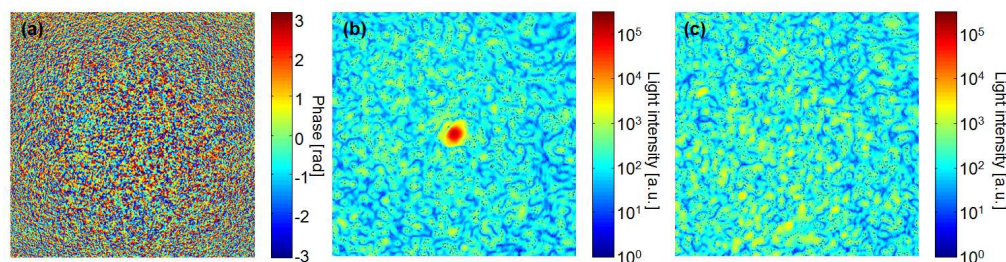
Fig. 7. (a) The DOPC measured phase profile. (b) DOPC reconstructed signal. The field of view is ~12 μm. (c) Control measurement with the phase of the SLM set to 0.

5.1 Experiment

We employed the setup shown in Fig. 4 for the demonstration. To prepare a random scattering sample, we first dried a mixture of polystyrene microspheres of different diameters (0.2, 0.5, 1, 3, 5, 10 μm) with equal weight percentage in a water suspension on a cover glass.

We then added immersion oil on top of the microspheres and covered them with another cover glass. The quantity of $\mu_s l$ can be determined by measuring the transmitted ballistic light. Experimentally, we used a collimated laser beam 1 mm in diameter to illuminate the sample. The transmitted light was directed through an iris 1 mm in diameter placed 3 meter away from the sample and was measured with a power meter (Newport 1830). To avoid overestimation of $\mu_s l$ due to refraction, we used a mirror to slightly adjust the propagation direction of the transmitted light to ensure that the ballistic component entered the iris. Through the ballistic light measurement, we determined $\mu_s l$ ~13. The scattering sample was mounted on a translation stage and inserted between the two objectives. The experiments were performed in three steps. In step 1, we measured the wavefront of the beam propagating through Lens 1, the sample and Lens 2. In step 2, we enabled the DOPC system by displaying the correct phase profile on the SLM. In such a case, the DOPC output should retrace the scattering path through the sample and become a collimated beam. In step 3, we disabled the DOPC system by setting the phase of the SLM to 0 (no phase modulation) and measured the transmission of the disabled DOPC output through the sample. We expected to observe a random scattering pattern since the beam entering Lens 2 is approximately a plane wave.

5.2 Results

Figure 7(a) is the measured wavefront of the beam propagating from Lens 1 to Lens 2. The random scattering inside the sample severely distorted the spatial phase profile. Figure 7(b) shows the transmission of the enabled DOPC output. In such a case, the phase conjugate wave retraced its way through the scattering medium and became a collimated beam. The FWHM of the reconstructed signal is ~0.43 micron that is greater than the diffraction limited resolution (0.23 micron). In Fig. 7(c), we showed the transmission of the disabled DOPC output through the sample. Since the disabled DOPC output is approximately plane wave that is not matched to the phase profile of the sample, the transmission displays a random scattering pattern. The measured peak to background ratio in Fig. 7(b) is ~600. According to Ref [3,25], the peak to background ratio is a direct measure of the optical degrees of freedom. The number of independent optical modes was estimated from the measured phase profile [Fig. 7(a)] to be ~1000, which is reasonably in agreement with the measured peak to background ratio.

6. The impact of phase error on the process of optical phase conjugation through a random scattering medium

We can reasonably expect that the effectiveness of OPC through a scattering medium to reconstruct an initial input field should depend on the accuracy by which the phase conjugate field is produced. The exact relationship between fidelity and reconstruction efficiency is important and relevant as it can guide us in making informed design choices in OPC-based applications. However, this relationship is difficult to study experimentally with conventional OPC methods as it is difficult to controllably introduce errors into the phase conjugate fields. The DOPC system affords us an easy and well controllable means for introducing known phase errors into the OPC wavefront. We can simply add the desired phase shifts into the DOPC wavefront that the SLM generates.

In this section, we report on the theoretical analysis and experimental verification of the deterioration of the OPC reconstruction signal through a scattering medium when phase errors are present in the OPC wavefront.

The scenario is as follows. Consider an initial single optical mode incident on a random scattering medium. Suppose the medium is of sufficient thickness so that the transmitted light is composed of a large number of uncorrelated optical modes. If we record the phase profile of this transmitted field and return an OPC field that has a phase profile of opposite sign, we can expect to obtain an optimal reconstruction OPC signal when the OPC field is retransmitted through the scattering medium. If, instead, we introduce random phase errors into the OPC wavefront, we can expect the reconstructed OPC signal to diminish in strength. This section aims to address the exact deterioration relationship.

6.1 Theory

More formally, the scenario described above can be expressed mathematically as follows. The transmission of optical wave through random scattering media can be described with a transmission matrix t [3]. Suppose a single optical mode $E_a|a\rangle$ is incident on a random scattering medium where E_a is the complex amplitude of mode $|a\rangle$. Its transmission can be described by $\sum_b E_a t_{ba}|b\rangle$ wherein $|b\rangle$ represents a transmitted free propagating mode. Its phase conjugation is therefore $\sum_b E_a{}^* t_{ba}{}^*|b\rangle$. If the phase conjugation wave propagates back through the scattering medium, the complex amplitude of the reconstructed mode $|a\rangle$ becomes $E_a{}' = \sum_b E_a{}^* t_{ba}{}^* t_{ab}$. Due to reciprocity, we have $t_{ab} = t_{ba}$ and hence $E_a{}' = E_a{}^* \sum_b |t_{ba}|^2$. If a random phase error is present in the phase conjugation wave, the complex amplitude of the reconstructed mode $|a\rangle$ becomes $E_a{}'' = E_a{}^* \sum_b |t_{ba}|^2 \exp(i\phi_b)$ wherein ϕ_b represent a random phase error in mode $|b\rangle$. The power ratio of the imperfect OPC signal to the perfect OPC signal is therefore,

$$R_{power} = \left| \frac{E_a{}''}{E_a{}'} \right|^2 = \left| \frac{\sum_b |t_{ba}|^2 \exp(i\phi_b)}{\sum_b |t_{ba}|^2} \right|^2 . \tag{1}$$

To evaluate Eq. (1), we assign a random number to each ϕ_b ranging from $-\phi_{range}/2$ to $\phi_{range}/2$ (uniform probability distribution) and assume that $|t_{ba}|^2$ obeys a negative exponential distribution since the transmitted light through a sufficiently thick random scattering medium appears as a speckle pattern [26]. The calculated result is shown in Fig. 8 (dark line). Surprisingly, this model predicts that the reconstructed OPC signal decreases rather slowly with increasing phase errors. Even when ϕ_{range} reaches π such that the phase error is a random number between -π/2 and π/2, the reconstructed OPC signal would still be ~40% of its peak value (when no phase error is present). In the above analysis, the input signal is a single optical mode. Using the transmission matrix theorem, we can also study the case when the input signal consists of multiple optical modes (an image). Numerical evaluation shows that the reconstructed image has the same dependence on phase error as shown in Fig. 8 (dark line).

6.2 Experiment

To experimentally verify the theoretical prediction, we used a random scattering medium with $\mu_s l\sim 10$ as the sample. The experimental procedure is the same as described in Section 5. We first performed DOPC to reconstruct the input signal and measured the strength of the reconstructed signal. We then added random phase error digitally to each mode of the generated phase conjugate wave and gradually increased the range of the phase error ϕ_{range} while observing the OPC signal peak intensity variation. The experimental results are summarized in Fig. 8 (solid blue square), which agrees well with the theoretical prediction.
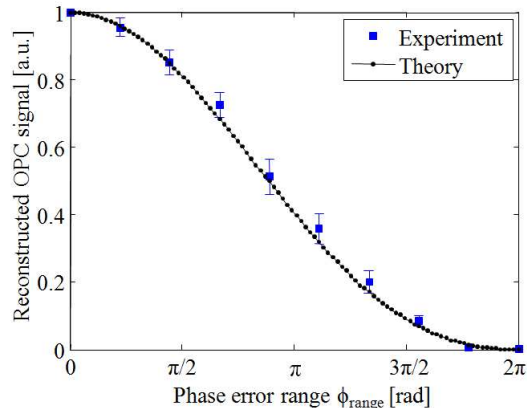
Fig. 8. Theoretical calculation and experimental measurements of the reconstructed OPC signal dependence on the amount of phase error.

6.3 Significance

The theoretical and experimental results prove that the reconstruction of an original light field by OPC through random scattering media is robustly tolerant to phase errors. It suggests that phase accuracy can be reasonably sacrificed to improve other aspects of the experiments in many adaptive optics methods for OPC through random scattering media, such as the experiment speed. For example, to accurately modulate the phase profile over 2π, many pixels are required. Our finding suggests that binary phase shaping can be used to achieve a comparable level of OPC signals while greatly reducing the required pixel number and increasing the experiment speed.

7. Conclusion

In summary, we have discussed the principle, design, and implementation of our DOPC method, a novel and versatile technique for generating OPC waves. Comparing to conventional OPC methods that rely on nonlinear light-matter interactions, DOPC can work with both CW and pulsed laser systems of various wavelengths and power levels. One limitation of the DOPC method is that the update rate is determined by the speed of the wavefront measurement combined with the update rate of the SLM employed. With high-speed commercially available devices, it should be possible to achieve an update rate close to 1kHz – a speed that is slow compared to Brillouin scattering based OPC systems but that is significantly faster than methods based on commonly used photorefractive crystals, such as $BaTiO_3$.

A significant advantage of DOPC is that the phase conjugate reflectivity can be arbitrarily controlled since the phase conjugate power is independent of the input signal power. This property is a key advantage over nonlinear optics based OPC systems.

The degrees of freedom handled by DOPC ($\sim10^6$) are significantly greater than many adaptive optics systems, comparable to the pixel by pixel optimization method but with a much shorter measurement time.

Through theoretical analysis and experimental tests, we further find that DOPC in random scattering media is a surprisingly robust process against phase errors. This result suggests that phase accuracy can be reasonably sacrificed to improve other aspects of the experiments such as the speed and the degrees of freedom capacity. This finding is of significant importance to many adaptive optics based techniques. We expect DOPC to find a broad range of applications in biomedical optics.

Acknowledgement